

# SECOND GENERATION FERMILAB MAIN INJECTOR 8 GEV BEAMLINE COLLIMATION FINAL DESIGN, INSTALLATION AND COMMISSIONING

K. Hazelwood\*, P. Adamson, B. Babacan, K. Danison-Fieldhouse, R. Donahue, B. Flanagan, T. Funk, M. Galante, M. Kucera, C. Montiel, D. Morris, R. Neswold, P. Neville, F. Novak, C. Olsen, A. Saewert, M. Stec, A. Watts

Fermi National Accelerator Laboratory<sup>†</sup>, Batavia, United States

## Abstract

A novel transverse beam collimation system has been installed and commissioned in the Fermilab Main Injector 8 GeV beamline. The new collimation system compliments existing collimators and helps ensure the Fermilab Main Injector and Recycler accelerators are capable of handling the increased beam power promised from the Fermilab PIP-II upgrade, currently underway. This paper will present the final design and installation of the collimation system as well as initial results from its commissioning.

## INTRODUCTION

The Main Injector 8 GeV Beamline (MI8) allows for beam extracted from the Fermilab Booster to be injected into the Booster Neutrino Beamline (BNB), the Main Injector accelerator (MI), or the Recycler Ring (RR). Due to the limited aperture of the Recycler Ring, it is necessary to collimate transverse beam halo and tails before that beam is lost in an uncontrolled fashion at those aperture restrictions. Transverse beam collimators have been installed in MI8 since 2006; though, they are now undersized for the current beam flux being transmitted through the MI8 beamline [1–5]. A project has been underway since the spring of 2021 to design and install an additional collimator system in the MI8 beamline to better control the beam losses in downstream machines and handle the anticipated increase in beam flux after the PIP-II upgrade is completed [6, 7].

## FINAL DESIGN

An extensive alternatives decision process was undertaken to decide on the design for the second generation of MI8 collimators [7]. The final design utilizes two approximately 88 ton collimators each consisting of four jaws, with pairs dedicated to either horizontal or vertical motion [8]. Past collimator designs required moving multi-ton collimator bodies to restrict the beam aperture. This design instead moves approximately 98 lb 304 stainless steel jaws within the vacuum vessel itself. This allows for much smaller motors, faster movement of the jaws, fewer vacuum connections and more steel for radiation shielding. Invar steel plungers and small vacuum bellows connect each jaw to two synchronized stepper motors. Since the jaws are in vacuum, most heat dissipation occurs via conduction; thermal contact with

the surrounding vacuum vessel is made with AlBr conduction pads. Opposite the conduction pads are spring loaded roller bearings that ensure the jaw is kept in thermal contact. Each jaw has an aperture equal to  $\pm 5 \sigma$  of  $20 \pi$ -mm-mrad (95%, normalized) beam emittance at that location in the beamline lattice. Likewise, each jaw is machined with an upstream taper to match the beamline lattice beta function. Internal upstream and downstream masks provide additional shielding from secondary particle spray. Multiple layers of marble significantly reduce radiation doses to personnel from the activated collimator steel during tunnel accesses.

## PROTOTYPE

A one-jaw prototype was constructed to validate key design assumptions. The prototype consists of one full-size jaw inside a vacuum vessel, two motion motors, a 1 kW heater tape affixed to the inside jaw aperture, and thermocouples both inside and outside the vacuum. A vacuum window on one end enabled direct measurement of jaw position with a ruler during testing (Fig. 1). Tests confirmed repeatable jaw travel, expected thermal expansion, and sufficient heat transfer from the jaw to the vessel exterior. The only design change resulting from the prototype was swapping the jaw thermal-conduction pads from Cu to AlBr, which offers slightly lower thermal conductivity but markedly higher strength and reduced long-term wear [9].

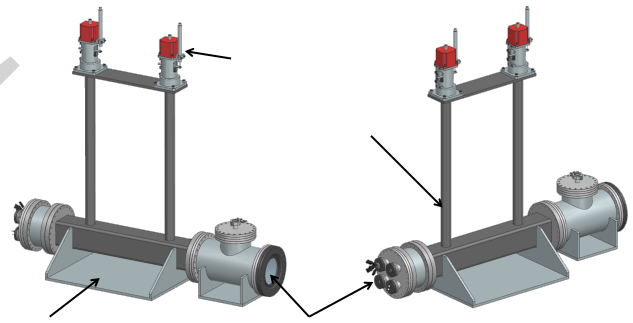


Figure 1: Illustration of the MI8 Collimator prototype test stand.

## INSTALLATION

Due to the size and complexity of the new MI8 collimators, the installation was done in stages.

\* kjh@fnal.gov

<sup>†</sup> This manuscript has been authored by Fermi Forward Discovery Group, LLC under Contract No. 89243024CSC000002 with the U.S. Department of Energy, Office of Science, Office of High Energy Physics.

### Preparation

In the summer of 2023, preparation of the collimator installation locations began. Modifications had to be made to the beamline vacuum, including the installation of additional ion pumps (IP) and new vacuum flanges for collimator mating. LCW headers and air lines had to be raised to allow for the large amount of transverse shielding in the new collimator design. 113 cables, totaling over 13.35 miles (21.5 km) in length, were pulled for the collimator installation. The new cables provide readings or control for 32 thermocouples (TC), 16 linear variable differential transformers (LVDT), 32 motor limit switches, 8 beam loss monitors (BLM), 4 IPs, 1 vacuum valve, and 16 stepper motors. Steel pads necessary to level the collimator installation and properly distribute the immense load were laid, aligned, anchored and grouted in-place at tunnel locations 825 and 827 to prepare for the laying of the collimator steel. Temporary beam pipe spool pieces were installed between flanges to allow resumed beam operation between installation stages.

### Jaw Connection Clevis Adapter Failure

Final installation of the new MI8 collimators began in summer 2024; about three-quarters of the steel had been placed when a component failure halted progress. While assembling the jaw vacuum assembly, an AIBr clevis adapter that attaches the motion plungers to the jaws broke in two during installation (Fig. 2). Due to the critical nature of this component, all clevis adapters were removed, inspected, and subjected to shear and torsion tests. The tests did not reveal any further defects in the sampled parts and suggested the break was due to a metallurgy anomaly in that single part. However, to prevent recurrence, the team replaced the AIBr fixtures with ones machined from stainless steel. It was decided that the increase in strength provided by making the clevis adapters from stainless steel was more significant than the additional thermal conductance provided by AIBr. The failure forced a pause for the rest of the year, during which the temporary beam-pipe spools were re-installed to resume beam operations that fall.



Figure 2: Failed jaw connection clevis adapter. Note the brittle appearance of the metal at the failure point.

### Final Installation

Final installation resumed summer 2025. The jaw vacuum assemblies were placed at the center of each collimator

station, and the remainder of the steel and marble shielding were stacked surrounding the vessels. Aluminium frames were used to capture and secure the marble plates. When possible, Al components were used on the collimator exterior. Al does not become as radio-activated; this reduces personnel exposure to highly activated components in the future (Fig. 3). A great deal of time was spent installing the motion control hardware components, testing movement and carefully terminating, connecting and securing cabling. Al frames, used to precisely position dedicated BLMs and also allow for quick removal and replacement of failed BLMs, were placed atop the finished collimators. Outside the tunnel, a motion control system consisting of a programmable logic controller (PLC) for reading out TCs and LVDTs and two independent stepper motor driver chassis, one for each collimator location, was installed [10].



Figure 3: New MI8 collimator installed at station 827, the other installation is seen in the distance at location 825.

## COMMISSIONING

Multiple commissioning studies were performed to validate the collimator installation before operational use.

### Motion Testing

All collimator jaws were driven with both local and remote controllers while being monitored in the tunnel. The jaws were driven to travel extremes to verify all hard stop and limit switches worked as expected, confirm that an accidental jaw skew was recoverable, calibrate the LVDT and motor step to travel readings, and verify that the expected full motion travel existed. While all tunnel hardware was found to work well, multiple issues were found with the remote stepper motor driving electronics. The issues were attributed to unreliable hardware and have since limited the use of the collimators to studies only while a permanent solution is under development.

### First Collimation

Despite the issues with the stepper motor controls, initial collimation tests were completed. The tests proved the collimators functional, that the jaw apertures were sufficient, and that there were no beam aperture obstructions (Fig. 4). Vacuum response to collimation was also monitored; no

degradation to vacuum during sustained collimation was observed.

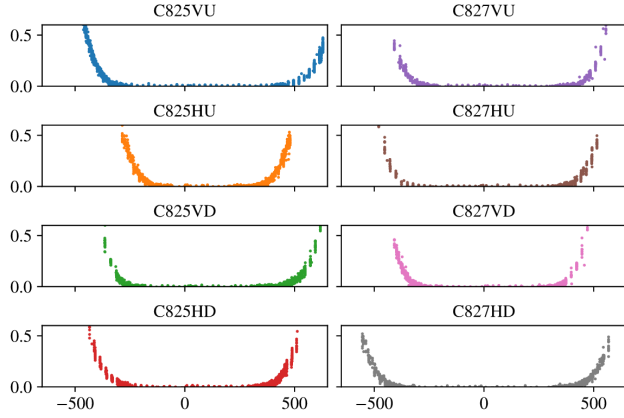


Figure 4: Protons lost vs jaw position. Flat regions show beam aperture with no obstructions.

### BLM Protons Loss Calibration

A dedicated BLM system, similar to one in place on the original MI8 collimators at tunnel locations 836 and 838, was installed for the new collimators as well [11]. Eight BLMs were installed, one above each jaw upstream peak collimation point. Having a BLM for each jaw allows for the attribution of protons lost and beam power lost per jaw. Studies were performed to determine the transfer matrix coefficients needed to estimate protons lost per BLM reading for each jaw (Fig. 5). Multiplying the eight live BLM readings by the inverse of the transfer matrix yields protons lost per jaw. These readings are actively monitored by the machine protection system (MPS). If any one BLM loss or calculated jaw proton loss exceeds expert defined limits, the beam is automatically disabled.

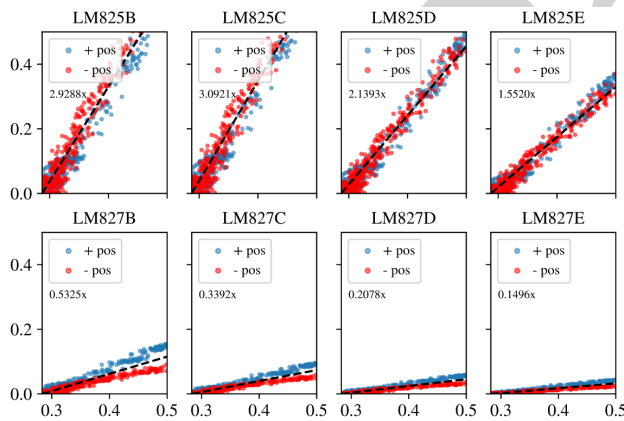


Figure 5: Jaw C825VU BLM loss readings vs protons lost.

### TC Response and Jaw Temperature Estimation

Using the prototype test data, the TC readings were fit to find each TCs thermal time constant,  $\tau$  (Fig. 6). Using the TC  $\tau$  values and the known heater temperature, the thermal resistance and capacitance of the jaws was estimated.

The jaw system was modeled as a linear (first-order, conduction dominated) two-state thermal process with input (beam) power and ambient disturbance. The internal jaw peak temperature is estimated via a discrete-time Kalman filter [12] using the external thermocouple measurements (Fig. 7). Using this model, MPS limits are set such that the beam is automatically disabled if any one TC reading exceeds values where the jaw temperature estimate is higher than desired. More work is planned to use the jaw temperature model along with the dedicated BLM proton loss calculation to continuously estimate the jaw temperature, detect anomalous TC readings or model estimate errors that may suggest the system has changed.

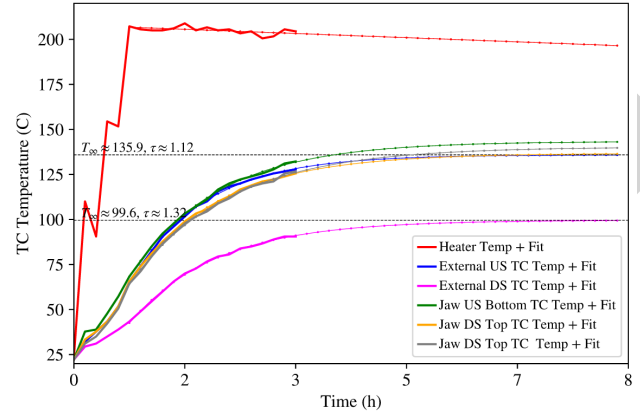


Figure 6: Prototype TC data thermal time constant fits.

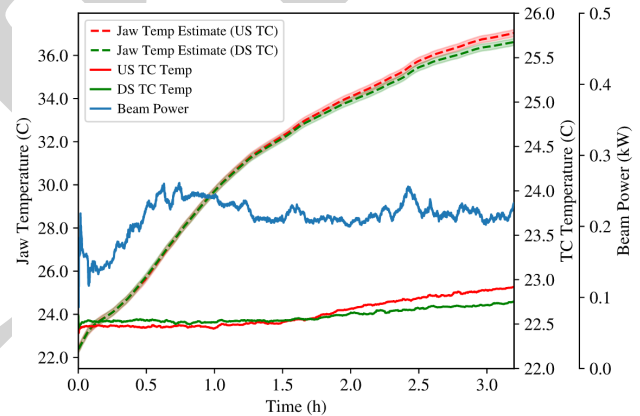


Figure 7: Beam study to test thermocouple response and tune jaw temperature estimation model.

## CONCLUSION

The new MI8 collimation system has been successfully installed and commissioned. Further work is underway to implement additional monitoring, machine protections and collimation tuning optimization techniques [13]. A new PLC based stepper motor driving system is under development and scheduled to be installed this summer to replace the hardware currently limiting the operational use of the collimators. The new MI8 collimators will be ready by fall 2026; in time for the long awaited resumption of beam operations in Main Injector [14].

## REFERENCES

- [1] B. C. Brown, D. Capista, I. Kourbanis, N. V. Mokhov, and V. Sidorov, "Collimation for the Fermilab Booster to Main Injector Transfer Line", *Conf. Proc. C*, vol. 070625, p. 1673, 2007. doi:10.1109/PAC.2007.4440860
- [2] B. C. Brown *et al.*, "Studies of beam properties and main injector loss control using collimators in the Fermilab booster to main injector transfer line", *Conf. Proc. C*, vol. 070625, p. 1670, 2007. doi:10.1109/PAC.2007.4440859
- [3] B. C. Brown, P. Adamson, D. P. Capista, D. K. Morris, and M.-J. Yang, "First results from MI8 collimator use", Rep., Jan. 2007. <https://beamdocs.fnal.gov/cgi-bin/sso/ShowDocument?docid=2618>
- [4] N. V. Mokhov, "Beam loss limits for collimation within the main injector tunnel", Rep., Jun. 2006. <https://beamdocs.fnal.gov/cgi-bin/sso/ShowDocument?docid=2359>
- [5] N. V. Mokhov and B. C. Brown, "MARS15 calculations for MI8 collimator design", Rep., Oct. 2006. <https://beamdocs.fnal.gov/cgi-bin/sso/ShowDocument?docid=2426>
- [6] M. Ball *et al.*, "The PIP-II conceptual design report", United States, Rep. FERMILAB-DESIGN-2017-01; FERMILAB-TM-2649-AD-APC 1516858, Mar. 2017. doi:10.2172/1346823
- [7] K. Hazelwood *et al.*, "Second Generation Fermilab Main Injector 8 GeV Beamline Collimation Preliminary Design", in *Proc. NAPAC'22*, Albuquerque, NM, USA, Aug. 2022, pp. 116–119. doi:10.18429/JACoW-NAPAC2022-MOPA29
- [8] B. Donahue, "MI8 collimators final design review, design", Rep., Dec. 2022. [https://beamdocs.fnal.gov/cgi-bin/sso/RetrieveFile?docid=8965&filename=mi8\\_collimators\\_fdr\\_design.pptx](https://beamdocs.fnal.gov/cgi-bin/sso/RetrieveFile?docid=8965&filename=mi8_collimators_fdr_design.pptx)
- [9] T. Funk, B. Donahue, and H. Goldenberg, "MI8 collimators prototype testing report", Rep., Jun. 2024. [https://beamdocs.fnal.gov/cgi-bin/sso/RetrieveFile?docid=8965&filename=mi8\\_collimators\\_prototype\\_test\\_report.pdf](https://beamdocs.fnal.gov/cgi-bin/sso/RetrieveFile?docid=8965&filename=mi8_collimators_prototype_test_report.pdf)
- [10] K. Hazelwood, "MI8 collimators motion control specifications", Rep., Aug. 2024. [https://beamdocs.fnal.gov/cgi-bin/sso/RetrieveFile?docid=8965&filename=mi8\\_collimators\\_motion\\_control\\_specifications.pdf](https://beamdocs.fnal.gov/cgi-bin/sso/RetrieveFile?docid=8965&filename=mi8_collimators_motion_control_specifications.pdf)
- [11] R. Goodwin, "MI-8 collimator loss monitors", Rep., Nov. 2010. [https://inteng.fnal.gov/Integrated\\_Eng/GoodwinDocs/pdf/LA%20docs/MI-8%20Loss%20Monitors.pdf](https://inteng.fnal.gov/Integrated_Eng/GoodwinDocs/pdf/LA%20docs/MI-8%20Loss%20Monitors.pdf)
- [12] A. P. A. Mohinder S. Grewal, *Kalman Filtering: Theory and Practice Using MATLAB*. 2nd Edition, John Wiley and Sons, Inc, 2001.
- [13] B. Babacan, R. Ainsworth, K. Hazelwood, and P. Snopok, "Optimizing collimator positions using bayesian optimization in the Fermilab MI-8 transfer line", in *Proc. IPAC'25*, Taipei, Taiwan, Jun. 2025, pp. 2711–2714. doi:10.18429/JACoW-IPAC2025-THPM012
- [14] K. Hazelwood *et al.*, "1 MW Beam Power in the Fermilab Main Injector", presented at IPAC'26, Deauville, France, May 2026, paper WEV4303, this conference,